

SYSTEM FOR AUTOMATED DESIGN BY PHYSICAL PROCESSES OF 3D MODELS IN A DRYING CHAMBER FOR HYGROSCOPIC MATERIALS

Yaroslav SOKOLOVSKYY^{*}, Oleksiy SINKEVYCH^{**}

^{*}Department of Computer-Aided Design Systems, Lviv Polytechnic National University,
79058, Ukraine, Lviv, str. Mytropolyta Andriya, 3

^{**}Department of Computer Science, Ukrainian National Forestry University,
79058, Ukraine, Lviv, str. Gen. Chuprynyk, 103

yaroslav.i.sokolovskyy@lpnu.ua, oleksiy1694@gmail.com

received 18 January 2024, revised 27 November 2024, accepted 28 December 2024

Abstract: Designing 3D models of drying chambers, especially of a new type, is a long and complex process. Nevertheless, the availability of 3D models of drying chambers allows for the necessary research before their actual design. In this paper, a software for the automated design of a 3D model of a drying chamber was developed to save time and material resources. To simulate the drying process of hygroscopic materials in this 3D model, an asynchronous cellular automaton model was developed. The software is the result of the programming implementation of several algorithms, including: an algorithm for automated design of a 3D model of a drying chamber using SolidWorks API tools; an algorithm for representing the 3D model under study as a cellular automaton field; an algorithm for calculating input data for simulation; an algorithm that uses transition rules for the asynchronous cellular automaton model; an algorithm for saving and displaying simulation results; and an algorithm for comparing simulation results. The software was verified and the mathematical models were validated using experimental data. The input data for the simulation were obtained from real technological conditions implemented in real drying chambers. The modeling results were used to obtain graphical dependencies of the desired material and drying agent parameters over time. The analysis of the results included their comparison with the data obtained by sensors in a real drying chamber. The relative error was determined, the average values of which did not exceed 13%, which confirms the accuracy of the results. In the long-term, the developed software has the potential to become a valuable tool in the design of new and more efficient drying chambers, offering opportunities for designing, modeling, and analyzing research results.

Key words: software, hygroscopic materials, cellular automaton field, SolidWorks API, modeling process

1. INTRODUCTION

In the rapidly advancing world of technology, it is essential not only to keep pace with changes but also to actively leverage cutting-edge information technologies to enhance traditional industries. This is particularly relevant to the modeling of the drying process of hygroscopic materials, such as wood, which has played a crucial role in the production of high-quality wooden products and materials for decades. This process also affects sectors such as construction, furniture manufacturing, and the packaging industry. In particular, the development of software for the computer-aided design of 3D models of drying chambers and the simulation of drying processes in them offers significant potential for increasing efficiency in these sectors.

Over the past decades, many efforts have been made to improve the design of drying chambers and increase their efficiency. Researches such as [1] and [2] emphasize the advantages of automating the design of drying chambers using modern software interfaces, in particular the SolidWorks API. In turn, research [2] focuses on the creation of simplified, operator-usable 3D models of drying chambers, while in [3], complex mathematical models developed to simulate heat and moisture exchange processes in such chambers. In addition, studies such as [4] address the problems of high-temperature drying, propose advanced mathematical

approaches, including the Navier-Stokes equation, to model the related heat, and mass transfer processes.

Despite these advances, traditional modeling methods remain computationally intensive, requiring significant time and computing resources. Nevertheless, recent studies [5] and [6] show that the cellular automata method can serve as a promising alternative, offering faster modeling without compromising accuracy. For example, in [5], finite element methods are compared with cellular automata for modeling wood drying, demonstrating comparable accuracy in a two-dimensional scenario, but with reduced computational expense. Similarly, in [6], asynchronous cellular automata were successfully applied to heat conduction problems, emphasizing their potential for high-speed computing in complex systems.

Even though cellular automata demonstrate high efficiency in modeling, the possibility of integrating them with 3D models of drying chambers is still insufficiently studied. This unsolved problem emphasizes the need for further research to develop innovative solutions. These solutions can improve the efficiency and accuracy of not only the computer-aided design of 3D models of new and potentially more efficient drying chambers, but also the simulation of the drying process in them.

The object of research in this work is the process of drying hygroscopic materials in drying chambers.

The subject of the study is a cellular automata model for simulating the drying process of hygroscopic materials in drying cham-

For the computer-aided design of the 3D model of the drying chamber, the following dimensions of the body were taken into

account: height 2.25 m, width 5.703 m, length 7.291 m, with a wall thickness of 5 cm, and parameterized dimensions (refer to Tab. 1).

Tab.1. Parameterized dimensions of the main components of the 3D model of the drying chamber

Component of the 3D model	A, mm	B, mm	C, mm	D, mm	E, mm	F, mm	G, mm	H, mm	I, mm	J, mm	K, mm	L, mm
Water heater	555	402	730	808	38	477	19	12.5	-	-	8	-
Axial fan	47.74	740.83	54.43	638.53	743.94	843	766.8	-	-	-	-	-
Humidifying nozzle	55	25	15	30	14	-	-	-	-	-	-	-
Ceiling	4848	477	5703	5058	7291	242.5	1003	2365.5	347.5	547.5	3438.5	238.5

Hence, during automated design, it is essential to utilize the primary window of the software, as depicted in Figure 2. Within this window, users can specify the nominal dimensions of the hygroscopic material, its species, and the quantity per stack. In this case, 16 stacks are designed, each containing 36 pine lumber with a thickness of 32 mm, a width of 75 mm and a length of 2.5 m. The height of the spacer between rows in the stack is automatically determined based on the height of the hygroscopic material.

ed 3D models are stored in the program directory by default, though users can easily customize this location in the software settings.

Through automated design, a 3D model of the drying chamber in SolidWorks can be obtained, as illustrated in Figure 4. The use of the SolidWorks API significantly saves time on this task.

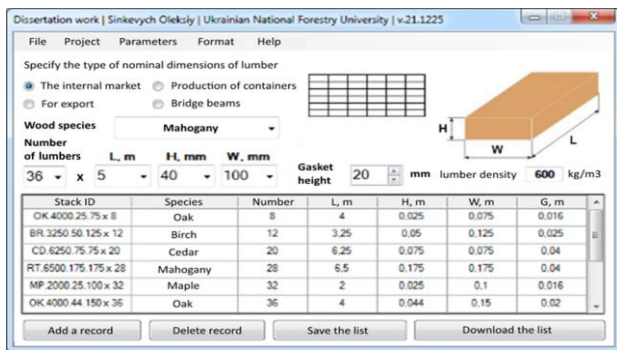


Fig. 2. View of the main window of the developed software

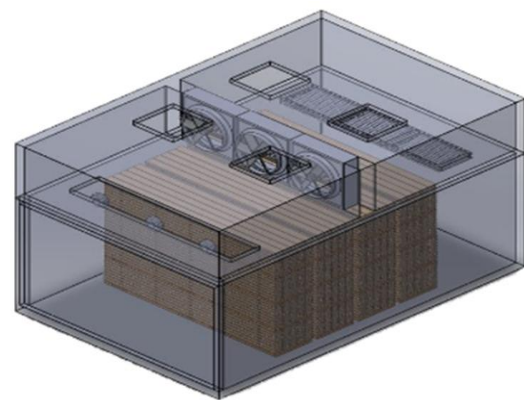


Fig. 4. General view of the drying chamber assembly in SolidWorks

Upon selecting all the requisite parameters and clicking the "Add a record" button, a new stack identifier is appended to the database. Its ID is constructed in the following manner: the initial two letters denote the wood species code, such as "BR" for birch, "CD" for cedar, "RT" for mahogany, "MP" for maple, "OK" for oak, and so forth. The subsequent numbers correspond to the length, height, and width of an individual material, along with their quantities. This comprehensive information is crucial for the automated design of the specified stack.

3. CREATION OF A CELLULAR AUTOMATA FIELD

To create a cellular-automata field, the initial step involves creating a specific graphic scheme (refer to Fig. 5), that illustrating the systematic process of transforming the 3D model of stacks. Similarly, the process of converting the 3D model of the drying chamber will take place.

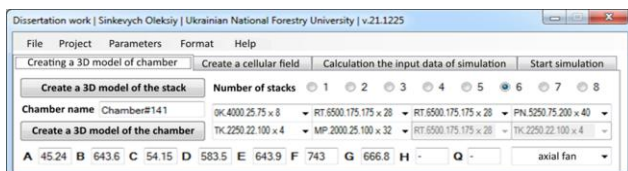


Fig. 3. Tab of the automated design of the 3D model of the drying chamber

However, real drying chambers commonly incorporate multiple stacks. In light of this, the software's first tab (refer to Fig. 3) was developed. This tab enabling users to specify the number of stacks and choose their type from the list created in the main program window (as described earlier). In essence, the user has the option to facilitate the automated design of either a 3D model of individual stacks or an entire assembly of the drying chamber. When opting for the entire assembly, it is necessary to define its name. All creat-

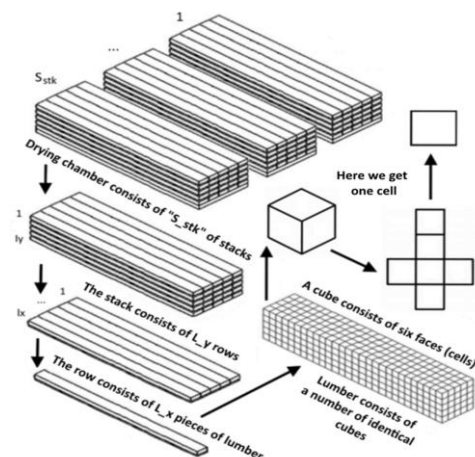


Fig. 5. Scheme of transformation of a 3D model of stacks into a three-dimensional array of cells

The creation of a cellular automata field [9] involves the following steps:

1. The program retrieves the dimensions of the dried materials in stacks, including "L" for length, "H" for height and "W" for width.
2. The program retrieves the maximum allowable division density of the 3D model (d_m), calculated across the greatest common divisor among its dimensions.
3. The program retrieves the desired level of division (d), indicating the precision of the calculations. Higher levels of division result in increased time and resource expenditure.
4. The program determines the final division density (d), which

defines the cell sizes. All cells possess identical face dimensions.

5. The program reads the number of drying materials in one stack (S_{imb}) and determines the number of materials in one row (l_x) and the number of rows (l_y) in one stack. Additionally, the program reads the number of stacks (S_{stk}).
6. The program retrieves the total number of cells on the cellular automata field for each of the three coordinates (S_x, S_y, S_z).
7. The program creates a three-dimensional array (a), where the elements represent cells.
8. The program determines the type of each cell on the cellular automata field according to the algorithm (refer to Fig. 6).

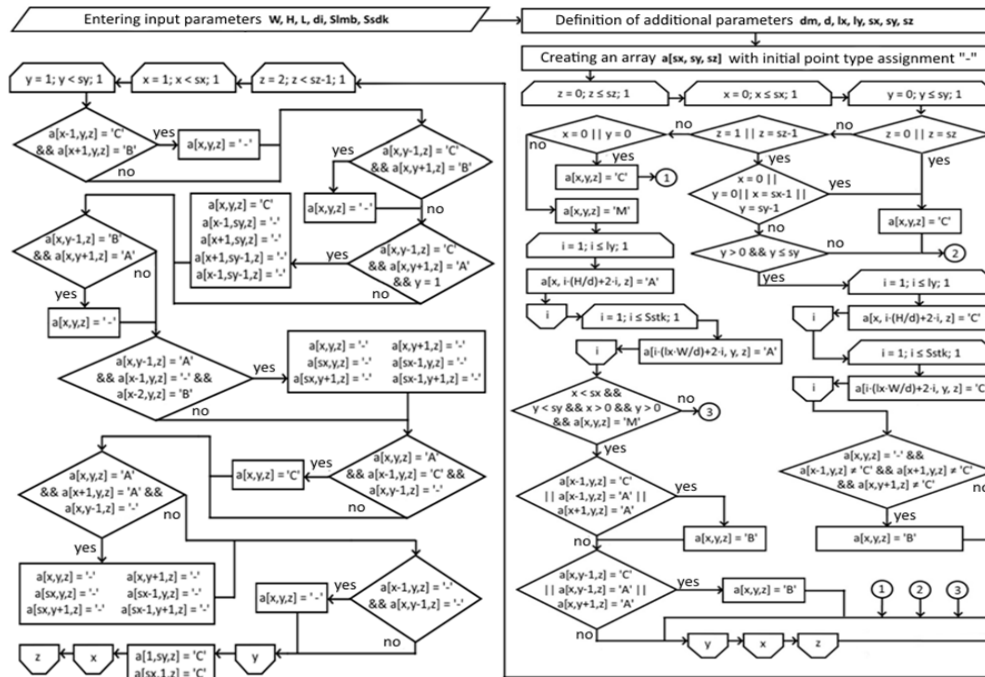


Fig. 6. Algorithm for creating a cellular automata field within stacks

When considering the cellular automata field within the arrangement of the stacks, the cells can have different types, with the main ones being: "A" for the drying agent, "B" for the border of lumber, and "M" for their internal drying zone. To create a cellular automata field by using the software, it is necessary to open the second tab of the main program window (refer to Fig. 7). On this tab, users can inspect the structure of this cellular automata field. To do so, they need to specify one of the coordinates and click the "Check" button. The two-dimensional view of this field will be display in the window below.

The structure of each cell contains information about its moisture content, temperature, coordinates (location), and time. The inclusion of time allows for the observation of changes in all cell parameters over time, a crucial aspect when generating graphic dependencies for a specific cell. Simultaneously, the upper-left vertex of the selected cell determines the coordinates of its location.

Considering the cellular automata field for the entire 3D model of the drying chamber, the cells have the following designations: "G" for the area of humidifying nozzles, "N" for the area of supply-exhaust channels, "V" for the area of axial fans, "H" for the location of water heaters, and "W" for the walls, ceiling, and chamber ceiling. These new designations enable the application of additional transition rules, particularly when the drying agent interacts with various components of the 3D model of the drying chamber. Such a cellular automata field is finite and constitutes one of the two parts of the cellular automata model. However, it's crucial to consider the computational capabilities of computer equipment during its creation. Although fewer resources are utilized compared to the finite difference method (one cell replaces four points), the required resources for its creation remain substantial. Consequently, the constructed cellular automata field accurately replicates the assembly structure of the designed 3D model of the drying chamber (refer to Fig. 8).

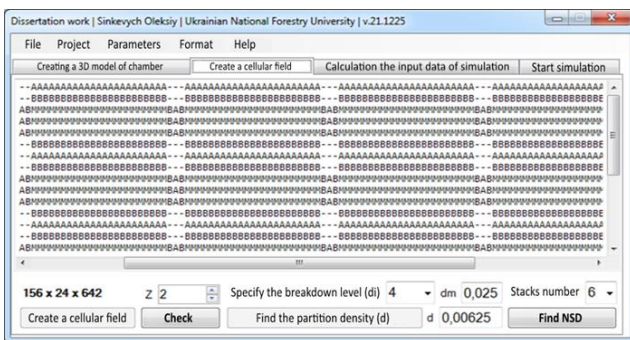


Fig. 7. Tab of the cellular automata field creation

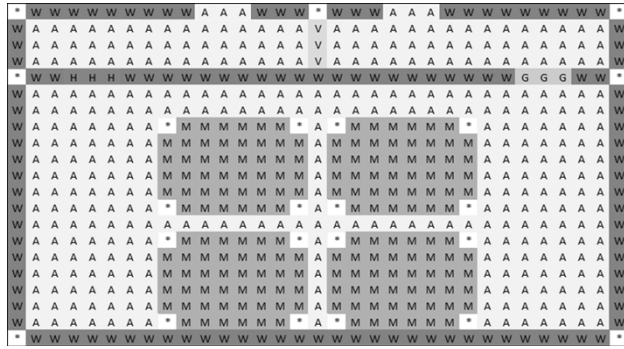


Fig. 8. View of the created cellular automata field

4. ANALYSIS OF MATHEMATICAL MODELS OF HEAT AND MASS TRANSFER PROCESSES IN DRYING CHAMBERS

To create transition rules, it is imperative to initially analyze the pertinent mathematical models describing the heat and mass transfer processes during the drying of hygroscopic materials [10-14]. Those mathematical models must consider the impact of various components of the drying chamber on alterations in the parameters of the drying agent, as well as its influence on the dried material. Additionally, it is advisable to incorporate the influence of the temperature of the walls of the drying chamber and the heater on the temperature of the drying agent. Furthermore, it is crucial to consider the impact of humidifying nozzles on the relative humidity content of the drying agent. Another important task is involves determining the initial speed of movement of the drying agent, a parameter influenced by the characteristics of the axial fans and their quantity.

To modeling the drying process of hygroscopic materials, it is essential to consider the heat transfer among various components within the system. In this context, hygroscopic materials act as the heating object, with water heaters performing as the heat source. The drying agent enables the transfer of heat between them. Unfortunately, the walls, roof, and ceiling absorb a portion of the heat from the drying agent that has traversed from the heaters to the hygroscopic materials. Consequently, it is possible to make certain simplifications by treating all components contributing to heat loss as a unified entity, denoted by a general temperature, T_w . In essence, the heat exchange, as described above, incorporates the heat balance equation [15] for the heater, drying agent, and other components of the drying chamber, and taking the following form:

$$C_h N_h m_h \frac{\partial T_h(x,y,Fo)}{\partial Fo} + N_g G_p I_p + L_{in} (C_n + C_p \varphi_n) T_n - G_0 \frac{\partial U_m(x,y,Fo)}{\partial Fo} - \frac{Nu_q \lambda_a}{r l} (T_a(x,y,Fo) - T_m(x,y,Fo)) - C_w m_w \frac{\partial T_w(x,y,Fo)}{\partial Fo} - L_{out} (C_n + C_p \varphi_a(x,y,Fo)) \cdot T_a(x,y,Fo) = \left(\frac{0.622 V_a P_{bar}(x,y,Fo) (1 + \varphi_a(x,y,Fo)) C_a}{R(273 + T_a(x,y,Fo)) (0.622 + \varphi_a(x,y,Fo))} + m_w C_w \right) \frac{\partial T_a(x,y,Fo)}{\partial Fo}, \quad (1)$$

where: P_{bar} – barometric pressure, V_a – volume of the drying agent, φ_a – relative humidity of the drying agent, L_{out} – the quantity of moist air leaving the chamber through inlet-exhaust channels, m_w – mass of all components of the drying chamber that absorbing heat from the drying agent, except for the hygroscopic material, T_w – temperature on the surface of these components, C_w – average specific heat capacity of materials for all of those components, T_m –

temperature of the hygroscopic material, T_a – temperature of the drying agent, l – size of the hygroscopic material along the movement of the drying agent, r – specific heat of vaporization, λ_a – coefficient of thermal conductivity of air, Nu_q – Nusselt heat transfer criterion, U_m – moisture content of the hygroscopic material, G_0 – mass of absolutely dry hygroscopic material, T_n – temperature of fresh air, φ_n – relative humidity of fresh air, C_p – specific isobaric heat capacity of water vapor, C_n – specific isobaric heat capacity of incoming fresh air, L_{in} – quantity of fresh air entering through inlet-exhaust channels, I_p – enthalpy of 1 kg of water vapor, G_p – quantity of water vapor entering the system through the humidifying nozzle, N_g – number of humidifying nozzles, Fo – Fourier number, T_h – temperature of the surface of the water heaters, m_h – mass of one water heater, N_h – number of water heaters, C_h – specific heat capacity of the metal of the water heaters, R – the universal gas constant, C_a – the specific isobaric heat capacity of the drying agent.

$$C_1 \alpha_t S_t (T_t - T_h(x,y,Fo)) - C_2 \alpha_h S_h (T_h(x,y,Fo) - T_a(x,y,Fo)) = C_h m_h \frac{\partial T_h(x,y,Fo)}{\partial Fo}, \quad (2)$$

where: S_h – heating surface area of the water heaters, α_h – coefficient of heat transfer of the cylindrical surface of the heaters, C_2 – coefficient of the thermal release surface state of the heaters, T_t – temperature of the heat carrier (hot water) in the heaters, S_t – surface area of heat transfer of the hygroscopic material, α_t – coefficient of heat transfer from condensing water vapor to the internal surface of the heaters, C_1 – coefficient of thermal losses of the heaters.

$$\alpha_w (T_a(x,y,Fo) - T_w(x,y,Fo)) - \alpha_s (T_w(x,y,Fo) - T_n) = C_w \rho_w l_w \frac{\partial T_w(x,y,Fo)}{\partial Fo}, \quad (3)$$

where: l_w – dimension of the wall along the movement of the drying agent, ρ_w – average density of wall materials, considering heat insulation layers, α_s – coefficient of heat transfer from the external surface of the walls to the external environment, α_w – coefficient of heat transfer of the drying agent with components of the drying chamber absorbing heat from it, except for the hygroscopic material.

$$Nu_q = 0.0641 Re^{0.8} Gu^2 Pr^{0.333}, \quad (4)$$

where: Pr – Prandtl criterion, Gu – Guhman criterion, Re – Reynolds criterion.

In turn, the moisture balance equation in the drying chamber [14, 15] can accommodate changes in the relative humidity of the drying agent, which changes with its temperature. Essentially, this equation can be formulated as follows:

$$N_g G_p + L_{in} \varphi_n - \frac{Nu_m \lambda_a}{r l} (T_a(x,y,Fo) - T_m(x,y,Fo)) - L_{out} \beta_a \varphi_a(x,y,Fo) = \frac{\partial \varphi_a(x,y,Fo)}{\partial Fo} \cdot \frac{0.622 V_a}{R(273 + T_a(x,y,Fo))} \cdot \frac{P_{bar}(x,y,Fo)}{\varphi_a(x,y,Fo)^2 + 1.622 \varphi_a(x,y,Fo) + 0.622}, \quad (5)$$

where: β_a – coefficient of moisture transfer, Nu_m – Nusselt's mass transfer criterion, determined according to A.V. Nesterenko [16].

$$Nu_m = 0.027 Re^{0.9} Gu^{0.175} Pr^{0.333}, \quad (6)$$

According to the law of conservation of energy, the quantity of heat expended on heating and evaporating moisture from the hygroscopic material will always be equivalent to the amount of heat entering it [17]. For this, the heat balance equation within the hygroscopic material being dried can be employed, witch having

the following form:

$$\frac{\partial T_m(x,y,Fo)}{\partial Fo} = (1 + \varepsilon KoPnLu) \left(\frac{\partial^2 T_m(x,y,Fo)}{\partial x^2} + \frac{\partial^2 T_m(x,y,Fo)}{\partial y^2} \right) - \varepsilon KoLu \left(\frac{\partial^2 U_m(x,y,Fo)}{\partial x^2} + \frac{\partial^2 U_m(x,y,Fo)}{\partial y^2} \right), \quad (7)$$

At the same time, the moisture content of the hygroscopic material being dried is determined as follows:

$$\frac{\partial U_m(x,y,Fo)}{\partial Fo} = Lu \left(\frac{\partial^2 U_m(x,y,Fo)}{\partial x^2} + \frac{\partial^2 U_m(x,y,Fo)}{\partial y^2} \right) - LuPn \left(\frac{\partial^2 T_m(x,y,Fo)}{\partial x^2} + \frac{\partial^2 T_m(x,y,Fo)}{\partial y^2} \right) \quad (8)$$

where: Lu – Luykov criterion, which reflects the ratio of the convective diffusion coefficient (a_m) to the heat diffusion coefficient (a_q), Pn – Posnov criterion, which reflects the relationship between the intensity

of thermodiffusion ($\delta\Delta T_m$) to moisture diffusion transport (ΔU_m), Ko – Kosovych criterion, which represents the dependence between the amount of heat expended on evaporating liquid from the hygroscopic material ($r\Delta U_m$) to the amount spent on its heating $C\Delta T_m$, ε – phase transition coefficient.

Thus, the aforementioned equations constitute a mathematical model of the heat and mass transfer process within the drying chamber. This model allows the determination of the relative humidity and temperature of the drying agent, along with the moisture content and temperature of the hygroscopic material. Similar to any mathematical model, it must incorporate boundary conditions. Given its intricacy, a dedicated diagram (refer to Fig. 9) was devised to illustrate the coordinates of all its borders.

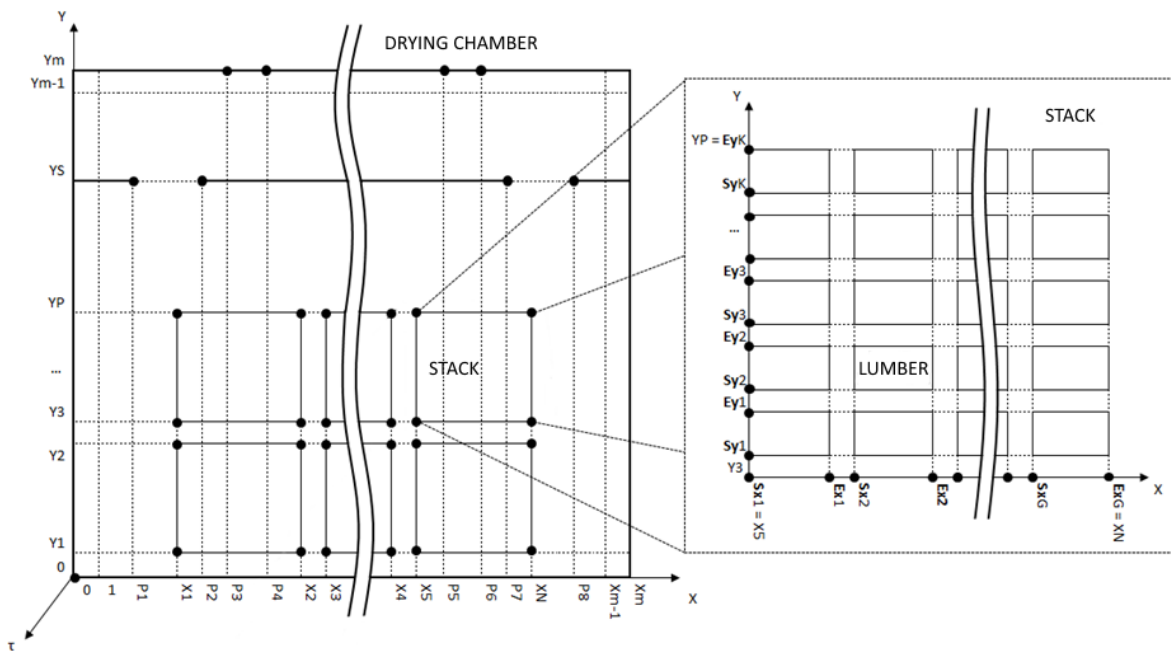


Fig. 9. The diagram illustrating the coordinates for the boundary conditions in the mathematical model

This diagram outlines the overall boundaries of the 3D model of the drying chamber. The X coordinate ranges from [0] to $[X_m]$, and the Y coordinate ranges from [0] to $[Y_m]$. The position of the supply and exhaust channels is determined by the Y coordinate $[Y_m]$, and X coordinates within $[P_3; P_4]$ and $[P_5; P_6]$. The point $[Y_s]$ defines the location of the overlap along the Y coordinate. The diagram also illustrates the placement of side passages containing humidifying nozzles (on the right) and water heaters (on the left). These passages have fixed values, with the Y coordinate $[Y_s]$ and X coordinates within $[P_1; P_2]$ and $[P_7; P_8]$, respectively.

It is crucial to specify the coordinates of the stack locations, which can change, and their precise $[X_n]$ and $[Y_p]$ coordinates can be determined when their quantity is known. The initial coordinates of the stack location always begin at $[X_1]$, and the end point of the X coordinate will be one step more $[+1]$ than the starting point, for instance, $[X_2]$. The height of one stack corresponds to the distance between points $[Y_1]$ and $[Y_2]$, while the distance between stacks is equivalent to the distance between points $[X_2]$ and $[X_3]$. Similarly, the width of one stack is equivalent to the length of the interval $[X_1; X_2]$.

The coordinates of the location points of hygroscopic materials within a specific stack can be determined using a similar principle. For

instance, the starting coordinate of the material location always begins with "S," and the ending one with "E." The subsequent letter indicates the selected coordinate. Thus, one material has a height equivalent to the interval $[S_{y1}; E_{y1}]$, and the width is equivalent to the interval $[S_{x1}; E_{x1}]$. Simultaneously, the height of one gasket between rows of hygroscopic materials is equivalent to the distance from point $[E_{y1}]$ to $[S_{y2}]$. Therefore, to initiate the drying process ($\tau = 0$), the following initial conditions, that characterizing the system's initial state, are introduced and have the following form:

$$T_m(x, y, 0) = 20^\circ C, \quad T_a(x, y, 0) = 30^\circ C, \quad T_w(x, y, 0) = 18^\circ C,$$

$$T_h(x, y, 0) = 70^\circ C, \quad T_t = 80^\circ C = const, \quad T_n = 10^\circ C = const,$$

$$U_m(x, y, 0) = 0.4 kg/kg, \quad \varphi_n = 0.6 kg/kg = const,$$

$$\varphi_a(x, y, 0) = 0.6 kg/kg, \quad \rho_s(x, y, 0) = 0.0173 kg/m^3$$

Due to the multitude of coordinates defining the locations of various boundaries, the 3D model segmented into three distinct zones, each with its specific set of boundary conditions. The first zone directly related to hygroscopic materials. It allows the deter-

mination of moisture content and temperature on the surface of a single hygroscopic material undergoing the drying process [12, 15, 16]. In this way, boundary conditions of this zone have the following form:

$$\left\{ \begin{aligned} \frac{\partial T_m(x_{b1}, y_{b1}, Fo)}{\partial x} &= (1 - \varepsilon)LuKoKi_m(Fo) - Ki_q(Fo), \\ \frac{\partial T_m(x_{b2}, y_{b2}, Fo)}{\partial y} &= (1 - \varepsilon)LuKoKi_m(Fo) - Ki_q(Fo), \\ \frac{\partial U_m(x_{b3}, y_{b3}, Fo)}{\partial x} &= Pn \frac{\partial T_m(x_{b3}, y_{b3}, Fo)}{\partial x} + Ki_m(Fo), \\ \frac{\partial U_m(x_{b3}, y_{b3}, Fo)}{\partial y} &= Pn \frac{\partial T_m(x_{b3}, y_{b3}, Fo)}{\partial y} + Ki_m(Fo), \end{aligned} \right. \quad (9)$$

where: Ki_m – Kirpichov's mass transfer criterion, reflecting the relationship between the liquid flow per length ($j(\tau)l$) to the density on the diffusion coefficient and the difference between the final and initial moisture content ($\rho\Delta U_m$), Ki_q – Kirpichov's heat transfer criterion, representing the dependence of the heat flow per length ($q(\tau)l$) to the thermal conductivity and the difference between the final and initial temperatures ($\lambda\Delta T_m$). In this case, the coordinates of the boundaries of this zone should be within the following limits:

$$\begin{aligned} &((x_{b1} \in [S_x, E_x], y_{b1} = E_y, y_{c1} = E_{y+1}) \cup (x_{b1} \in [S_x, E_x], y_{b1} = S_y, y_{c1} = S_{y-1})) \cap ((x_{b2} = S_x, y_{b2} \in [S_y, E_y], x_{c2} = S_{x-1}) \cup (x_{b2} = E_x, y_{b2} \in [S_y, E_y], x_{c2} = E_{x+1})) \cap (x_{b3} \in [S_x, E_x], y_{b3} = S_y \cup E_y) \cap (x_{b4} = S_x \cup E_x, y_{b4} \in [S_y, E_y]) \end{aligned}$$

The second zone pertains to the positioning of the stacks, where the hygroscopic material undergoing drying exposed to its drying agent. Alterations in the relative humidity and temperature of the drying agent can be assessed within this zone [13-15]. So, the boundary conditions for this zone have the following form:

$$\left\{ \begin{aligned} \frac{\partial T_a(x_{b5}, y_{b5}, Fo)}{\partial x} &= \frac{\alpha_m(x)(T_m(x_{b5}, y_{c5}, Fo) - T_a(x_{b5}, y_{b5}, Fo))}{Rv\rho_a C_a}, \\ \frac{\partial T_a(x_{b6}, y_{b6}, Fo)}{\partial y} &= \frac{\alpha_m(y)(T_m(x_{c6}, y_{b6}, Fo) - T_a(x_{b6}, y_{b6}, Fo))}{Rv\rho_a C_a}, \\ \frac{\partial \varphi_a(x_{b7}, y_{b7}, Fo)}{\partial x} &= \frac{\alpha_m(x)\rho_0(U_m(x_{b7}, y_{c7}, Fo) - U_p)}{Rv\rho_s(x_{b7}, y_{b7}, Fo)} - \frac{\partial \rho_s(x_{b7}, y_{b7}, Fo)}{\partial x} \frac{\varphi_a(x_{b7}, y_{b7}, Fo)}{\rho_s(x_{b7}, y_{b7}, Fo)}, \\ \frac{\partial \varphi_a(x_{b8}, y_{b8}, Fo)}{\partial y} &= \frac{\alpha_m(y)\rho_0(U_m(x_{c8}, y_{b8}, Fo) - U_p)}{Rv\rho_s(x_{b8}, y_{b8}, Fo)} - \frac{\partial \rho_s(x_{b8}, y_{b8}, Fo)}{\partial y} \frac{\varphi_a(x_{b8}, y_{b8}, Fo)}{\rho_s(x_{b8}, y_{b8}, Fo)}, \end{aligned} \right. \quad (10)$$

where: ρ_s – density of saturated vapor, U_p – equilibrium moisture content, ρ_0 – base density of materials, $\alpha_m(x)$, $\alpha_m(y)$ – moisture diffusion coefficients of materials, ρ_a – density of the drying agent, v – velocity of the drying agent flow, $\alpha_m(x)$, $\alpha_m(y)$ – heat transfer coefficients. In this case, the coordinates of the boundaries of this zone should be within the following limits:

$$\begin{aligned} &((x_{b5} \in [S_x, E_x], y_{b5} = E_{y+1}, y_{c5} = E_y) \cup (x_{b5} \in [S_x, E_x], y_{b5} = S_{y-1}, y_{c5} = S_y)) \cap ((x_{b6} = S_{x-1}, y_{b6} \in [S_y, E_y], x_{c6} = S_x) \cup (x_{b6} = E_{x+1}, y_{b6} \in [S_y, E_y], x_{c6} = E_x)) \cap ((x_{b7} \in [S_x, E_x], y_{b7} = E_{y+1}, y_{c7} = E_y) \cup (x_{b7} \in [S_x, E_x], y_{b7} = S_{y-1}, y_{c7} = S_y)) \cap ((x_{b8} = E_{x+1}, y_{b8} \in [S_y, E_y], x_{c8} = E_x) \cup (x_{b8} = S_{x-1}, y_{b8} \in [S_y, E_y], x_{c8} = S_x)) \end{aligned}$$

The last third zone encompasses the interaction of the drying agent with other components of the drying chamber. Within this

zone, it is possible to determine the relative humidity and temperature of the drying agent at its various boundaries, such as those in contact with walls, heaters, supply and exhaust ducts, etc. Consequently, the boundary conditions for this zone take on the following form:

$$\left\{ \begin{aligned} T_a(x_{b9}, y_{b9}, Fo) &= T_n, \\ T_a(x_{b10}, y_{b10}, Fo) &= T_h(x, y, Fo), \\ \varphi_a(x_{b11}, y_{b11}, Fo) &= \varphi_n, \\ \frac{\partial T_a(x_{b12}, y_{b12}, Fo)}{\partial x} &= -Bi_q(T_w(x_{b12}, y_{c12}, Fo) - T_a(x_{b12}, y_{b12}, Fo)), \\ \frac{\partial T_a(x_{b13}, y_{b13}, Fo)}{\partial y} &= -Bi_q(T_w(x_{c13}, y_{b13}, Fo) - T_a(x_{b13}, y_{b13}, Fo)), \end{aligned} \right. \quad (11)$$

where: Bi_q – the Bio heat transfer criterion reflects the ratio of the heat transfer coefficient from the body surface to the surrounding environment ($a_m l$) to the thermal conductivity coefficient of the body material (λ_m). In this case, the coordinates of the boundaries of this zone should be within the following limits:

$$\begin{aligned} &(x_{b9} \in [P_3, P_4] \cup [P_5, P_6], y_{b9} = Y_{m-1}) \cap \\ &\cap (x_{b10} \in [P_1, P_2], y_{b10} = Y_{s+1} \cup Y_{s-1}) \cap \\ &\cap (x_{b11} \in [P_3, P_4] \cup [P_5, P_6], y_{b11} = Y_{m-1}) \cap \\ &\cap ((x_{b12} \in (0, X_1) \cup (X_2, X_3) \cup \dots \cup (X_n, X_m), y_{b12} = Y_1, y_{c12} = 0) \cup (x_{b12} \in (0, P_3) \cup (P_4, P_5) \cup (P_6, X_m), y_{b12} = Y_{m-1}, y_{c12} = Y_m)) \cap ((x_{b13} = 1, y_{b13} \in (0, Y_m), x_{c13} = 0) \cup (x_{b13} = X_{m-1}, y_{b13} \in (0, Y_m), x_{c13} = X_n)) \end{aligned}$$

It is worth separately noting the influence of the number of axial fans and their power on the initial velocity of the drying agent. In this regard, it is important to consider the resistance of the stacks, which affects the initial velocity, and can be determined as follows:

$$v_0 = \frac{N_v P_v (1 - e_c)}{(1 - \frac{h_w}{h_w - h_g}) l_{st} h_{st} N_{st}} \quad (12)$$

where: N_{st} – total number of stacks, h_{st} – height of one stack, l_{st} – length of one stack, h_g – height of the spacer between rows of materials in a stack, h_w – height of one hygroscopic material, e_c – coefficient of expenditure during the operation of fans, P_v – power of fan, N_v – number of axial fans, v_0 – initial velocity of the drying agent.

5. DEVELOPMENT OF TRANSITION RULES FOR THE CELLULAR AUTOMATA MODEL

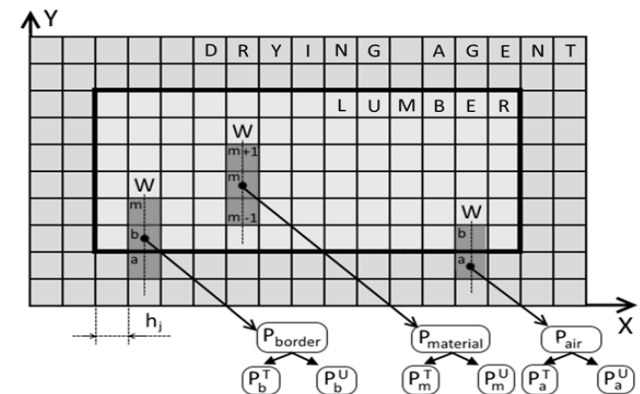


Fig. 10. Cell marking scheme used for transition rules

After analyzing the mathematical model, including its boundary and initial conditions, it becomes possible to formulate transition rules for the cellular automata model [17, 18]. The developed scheme (refer to Fig. 10) utilized to illustrate the conditional designations employed in these transition rules. It provides an example of the interaction among adjacent cells, where the interaction direction "W" corresponds to the Y coordinate.

In general, utilizing the cellular automata model involves the following steps:

- Establishing the direction of interaction "W" according to the normal distribution law;
- Start the iteration, equivalent to a time interval of Δt seconds;
- Choosing the target cell (mc) following the uniform distribution law;
- Verifying the type of neighboring cell (nc) and applying the relevant transition rules;
- Repeating steps 2-4 until all cells are selected;
- Finalizing the execution of the current iteration and assessing termination conditions;
- Concluding the simulation if the test is successfully completed;
- Advancing the simulation time and returning to step one if the test not met.

A satisfactory condition to finish modeling is reaching the specified simulation time or the desired moisture content of the hygroscopic material undergoing drying. The main transition rules have the following form:

IF 'mc' = «M»

AND 'nc' = «M» AND $P_m^T \neq P_{m+1}^T$ AND $P_m^U \neq P_{m+1}^U$

THEN $P_{m(new)}^U = P_m^U - C_1(P_{m+1}^U - 2P_m^U + P_{m-1}^U + \delta(P_{m+1}^T - 2P_m^T + P_{m-1}^T))$ AND $P_{m(new)}^T = P_m^T + C_2(P_{m+1}^T - 2P_m^T + P_{m-1}^T) + C_3(P_{m(new)}^U - P_m^U)$

IF 'mc' = «M»

AND 'nc' = «B» AND $P_m^T \neq P_b^T$ AND $P_m^U \neq P_b^U$

THEN $P_{m(new)}^U = P_m^U - C_1(P_b^U - 2P_m^U + P_{m-1}^U + \delta(P_b^T - 2P_m^T + P_{m-1}^T))$ AND $P_{m(new)}^T = P_m^T + C_2(P_b^T - 2P_m^T + P_{m-1}^T) + C_3(P_{m(new)}^U - P_m^U)$

IF 'mc' = «B» THEN $P_{b(new)}^U = (C_9(P_m^T - P_b^T) + a_j P_m^U + C_{10} P_a^U) / (a_j + C_{10})$ AND $P_{b(new)}^T =$

$= (P_a^T (C_5 - C_6 - C_4 \delta) + P_m^T (C_8 - C_7) - C_1 (P_m^U - P_a^U)) / (C_5 + C_8 - C_6 - C_7 - C_4 \delta)$

IF 'mc' = «A» AND 'nc' = «B» THEN $P_{a(new)}^T = P_a^T +$

$(C_{11} (P_b^T - P_a^T)) / C_{12}$ AND $P_{a(new)}^U = P_a^U + \frac{C_{13} (P_b^U - U_p)}{C_{14}} - \frac{P_a^U (P_n - P_s)}{C_{15} P_a^T} + \frac{P_a^U P_s P_{a(new)}^T}{C_{15} (P_a^T)^2} - \frac{P_a^U P_s}{C_{15} P_a^T}$

IF 'mc' = «A» AND 'nc' = «A» THEN

$P_{a(new)}^T = \frac{(P_a^T + P_{a+1}^T)}{2}$ AND $P_{a(new)}^U = \frac{(P_a^U + P_{a+1}^U)}{2}$

IF 'mc' = «A» AND 'nc' = «W» OR 'nc' = «V»

THEN $T_w = P_a^T$

IF 'mc' = «A» AND 'nc' = «H» THEN $P_{a(new)}^T = T_h$

IF 'mc' = «A» AND 'nc' = «N» THEN $P_{a(new)}^T = T_n$

IF 'mc' = «A» AND 'nc' = «G» THEN $P_{a(new)}^U = \frac{P_a^U + P_{a+1}^U}{2}$

Where the value of coefficients C₁-C₁₅ can be calculated as

follows:

$$C_1 = \frac{a_j \Delta t}{h_j^2}, \quad C_2 = \frac{\lambda_j \Delta t}{c_m \rho_m h_j^2}, \quad C_3 = \frac{\varepsilon \rho_0 r}{c_m \rho_m},$$

$$C_4 = a_j \rho_0 (1 - \varepsilon) \beta, \quad C_5 = \beta \lambda_j, \quad C_6 = \frac{a_j \lambda_j}{h_j}, \quad (13)$$

$$C_7 = \alpha_m a_j, \quad C_8 = \alpha_m \beta h_j, \quad C_9 = a_j \delta,$$

$$C_{10} = \beta h_j, \quad C_{11} = \alpha h_j, \quad C_{12} = v c_c \rho_c h_s,$$

$$C_{13} = a_j \rho_0 h_j, \quad C_{14} = v \rho_s h_s, \quad C_{15} = h_s \rho_s,$$

where: h_s – distance between hygroscopic materials in a stack and the gap between two stacks, c_c – specific heat capacity of the condensate, ρ_c – density of the condensate, δ – thermal gradient coefficient, ρ_m – density of materials, c_m – specific heat capacity of materials, λ_j – thermal conductivity coefficient of the material in the specified direction, h_j – size of one cell, Δt – time for one iteration. The value of j can be "1" for "x" and "2" for "y".

6. DEVELOPMENT OF THE DATABASE AND DISTRIBUTION OF ACCESS RIGHTS

To enter the input data of the simulation, it is necessary to open the third tab of the software (refer to Fig. 11).

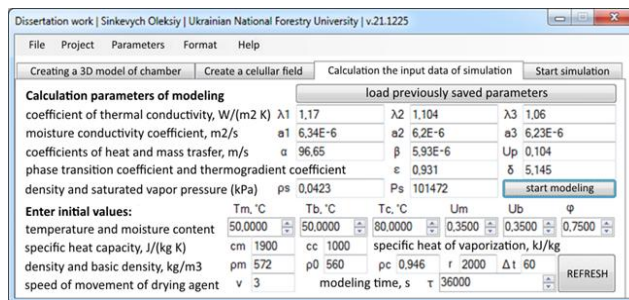


Fig. 11. Tab of the input data of the simulation and its launch

On this tab, the user enters the initial values of some parameters, in particular: temperature and moisture content of lumber; temperature and relative humidity of the drying agent; specific heat capacity; density and basic density of the material; specific heat of vaporization; simulation time and time step. At the same time, the rest of the parameters, most of which are represented by different coefficients, will be determined automatically. Having all the parameters for the simulation, user can start its execution using the same tab.

To carry out modeling, it is absolutely necessary to have a database in which the results will be stored. To create it, it was decided to use the MySQL Workbench Community Edition environment. The created database is named "dissertation" and consists of several interconnected tables, namely: "lumber", "stack", "chamber", "ca_field", "coefficients" and "results". The "lumber" table contains a unique lumber code that is generated automatically and has the following structure: "XX.LL.HH.WW", where "XX" is the type of wood (birch - "BR", cedar - "CD", Beech - "RT", maple - "MP", oak - "OK", pine - "PN", teak - "TK" and other), "LL" - length, "HH" - height, "WW" - width of lumber in mm. Also in this table there is information about the density of the material. The "stack" table contains a unique stack code that is generated automatically and has the following structure: "XX x LL", where "XX" is the number of lumber in the stack, and "LL" is

the unique lumber code. Also, this table contains data on the number of lumber in the stack, their location, and information on the size and number of spacers between rows of lumber. The "chamber" table contains the unique code of the drying chamber, which is generated automatically and has the following structure: "XX→SS", where "XX" is the number of stacks in the drying chamber, and "SS" is the unique code of the stack. Also, this table contains information about the number of stacks in the chamber and the scheme of their arrangement along it. The "ca_field" table contains information about the cell autofield, including the number and sizes of cells. The "coefficients" table contains information about all modeling parameters, both initial, which are constant, and current, which change with the passage of model time. The last table "results" contains information about the results of the simulation and is the largest among all of them. To display the entities, attributes and relationships between them, an Entity-Relationship (ER) diagram (refer to Fig. 12) was created. It provides an opportunity to better understand how the data will interact with each other in the developed software.

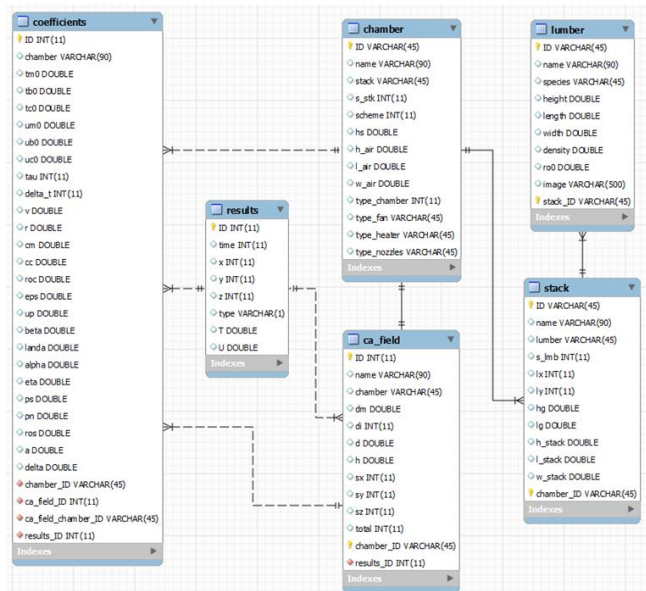


Fig. 12. View of the Entity-Relationship diagram for developed software

To visualize the functionality of the system from the perspective of users and other system agents, a UML use case diagram was created (refer to Fig. 13). It is used to describe how a system interacts with its environment, including users and various processes. By its structure, this diagram has actors that interact with the system. These actors are divided into 4 types, namely "Users", "SolidWorks experts", "Cellular automata experts" and "System administrators". Each of them has its own access rights and certain usage options. Each of these use cases represents a specific scenario that the system supports and can implement. At the same time, each scenario details the sequence of actions and interaction between actors and the system.

To visualize the interaction between system components within a specific usage scenario, a sequence diagram was created (refer to Fig. 14). It helps to understand the sequence of actions and the exchange of messages between different elements of the system involved in a specific process. In turn, this diagram shows three actors and their sequence of actions in the system.

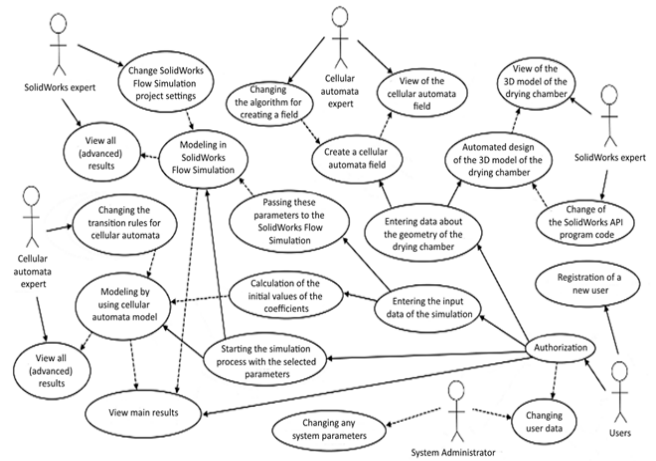


Fig. 13. View of the UML use case diagram

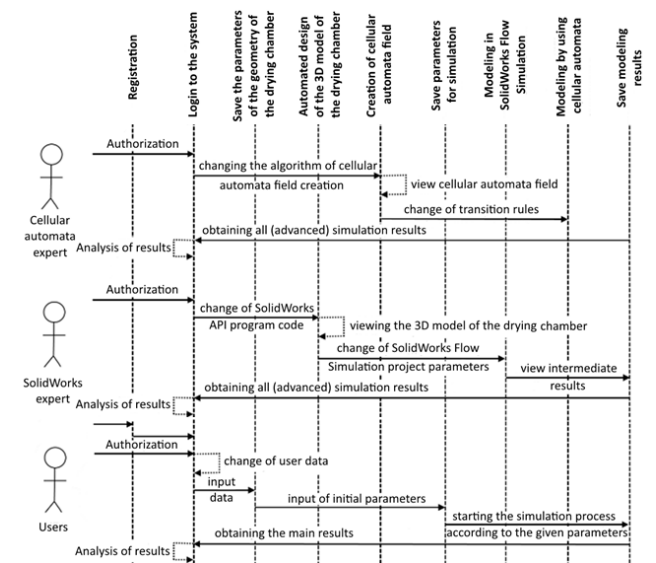


Fig. 14. View of the UML sequence diagram

7. SIMULATION OF THE DRYING PROCESS OF HYGROSCOPIC MATERIALS USING THE CELLULAR AUTOMATA MODEL

After initiating the simulation, an iterative cycle begins, executing transition rules among closely located cells. Through these interactions, the key parameters of both the drying agent and the hygroscopic material undergo changes. As illustrated in Fig. 15, influencing a single cell leads to subsequent alterations in 27 cells after several iterations. This approach effectively illustrates the cellular automata principle [18], where modifying values in specific cells, such as on material surfaces, directly influences internal cell values. To conveniently monitor temperature and moisture content changes in the drying material, users can utilize the "View values" window located in the "Format" section of the software's main menu.

This window helps user to view the changes of parameters in two-dimensional space on the cellular automata field, but for this, they need to specify the starting point of the tracking according to the coordinates (lower left corner of the field). After that, user can see cells that display a given parameter to choose from (temperature or moisture content). For the convenience of obtaining graphical dependencies, the values of the main parameters displayed in

the right part of the window. At the same time, user can select a specific area on the cellular automata field, thus obtaining the value of the desired parameter in space and time.

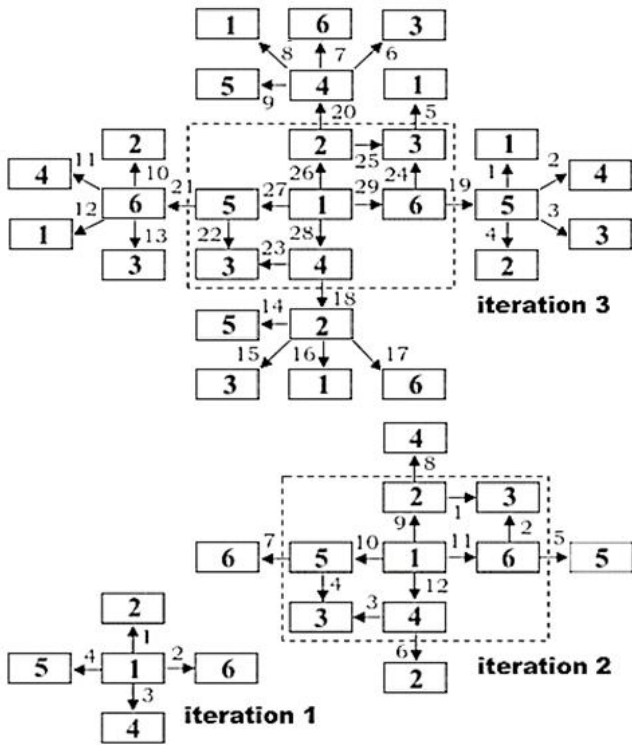


Fig. 15. Start of the iteration cycle

8. ANALYSIS OF THE OBTAINED SIMULATION RESULTS

As a result of the simulation [19], graphical dependences of the main parameters of the hygroscopic material to be dried and the drying agent over time were obtained (refer to Fig. 16 and 17). The main parameters include: the average relative humidity of the drying agent (P_a^U), the average temperature of the drying agent (P_a^T), the average moisture content of the hygroscopic material being dried in the stacks (P_m^U) and its average temperature (P_m^T).

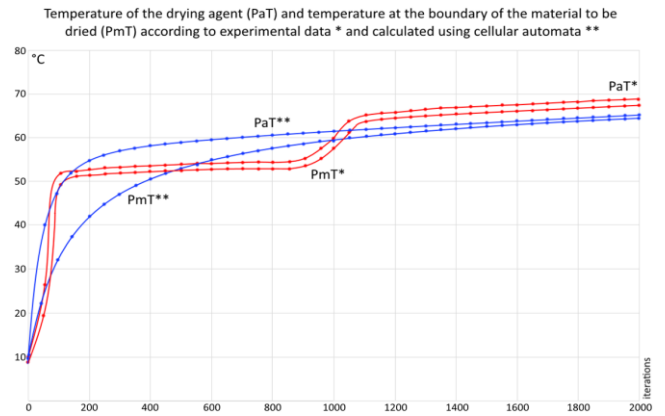
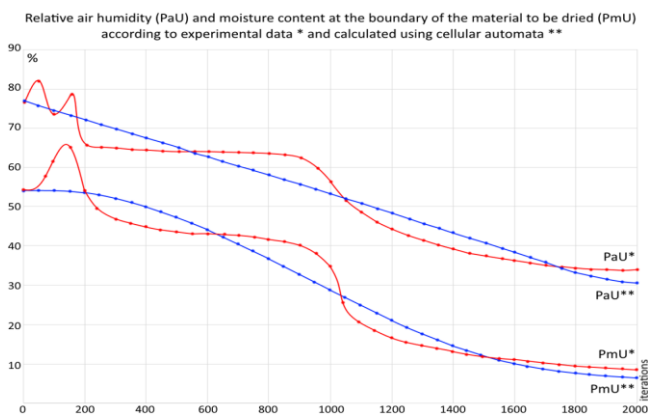


Fig. 16. A chart depicting the variation of the key parameters over time for the first study

To verify the obtained results, they compared with experimental data that obtained using the "LK-ZDR-100" wood drying chamber, located at "Rodors" LLC (Khmelytskyi region, Ukraine). Data for compared the first study collected using sensors between 29/10/18 and 06/11/18 for 30 mm thick pine material with an initial moisture content of 55%. Data for compared the second study collected between 18/03/23 and 01/04/23 for 45 mm thick pine material with an initial moisture content of 65%.

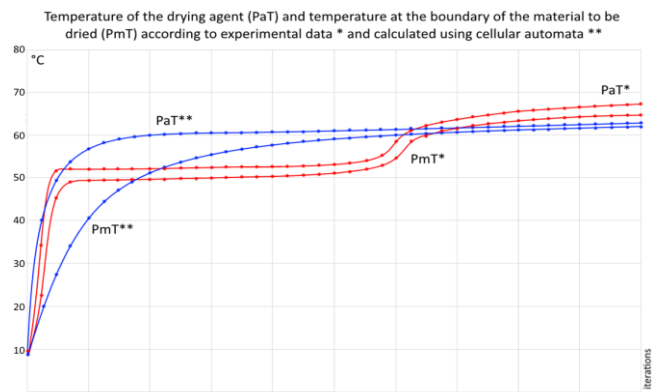
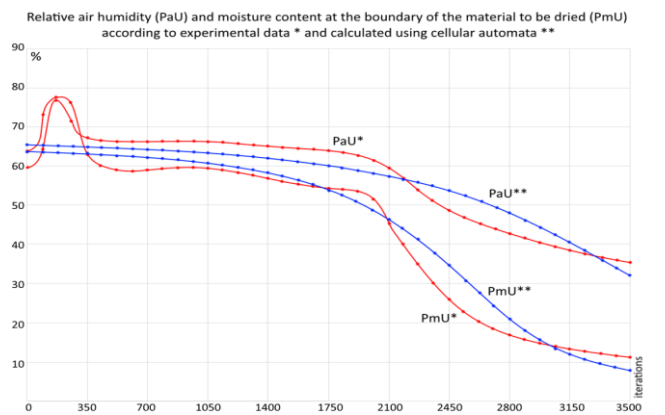


Fig. 17. A chart depicting the variation of the key parameters over time for the second study

The input parameters for comparing the results are as follows: initial relative humidity of the drying agent is 77% / 74%, the temperature of the heat carrier (hot water in the heaters) is 70 °C (for both data sets), the initial temperature of the drying agent is 15 °C / 19 °C, the initial temperature on the surface of the hygroscopic

material is 13 °C / 18 °C, the simulation time is 166 h / 291 h, and the iteration step is 300 s (for both data sets).

Visual evaluation of the results is important, but it doesn't provide a way to determine the accuracy of the modeling. In general, there are many ways to determine accuracy, each of which depends on the context and specifics of the comparative data [20]. In this case, two of the most common methods chosen to assess the accuracy, namely, the mean absolute error (MAE) and the mean absolute percentage error (MAPE). As a result of the calculations, the values of these errors were determined for the temperature and humidity parameters of the drying agent and hygroscopic material for both data sets.

It was established that the average value of MAPE is 13%. The largest values amounting to approximately 24%. This result may indicate that a limited number of cells of cellular automata field and limited transition rules between them were used in the initial phase of the simulation. Over time, the number of cells increases and the accuracy of the results improves significantly. Therefore, MAPE at the end of the simulation doesn't exceed 9%. This analysis confirms the accuracy and correspondence of the obtained results to real drying conditions. In addition, simulation results can be used to determine optimal input parameters for simulation in computational fluid dynamics programs, including SolidWorks Flow Simulation.

In general, the topic of this research is new. In this regard, the research results can be compared with related works of other authors, in particular, in work [3]. In this work, a three-dimensional mathematical model of heat and moisture transfer during drying of wood in drying chambers was developed. This model was successfully verified using numerical simulations and experiments, including the analysis of air movement and moisture. In turn, in [4] heat and mass transfer in the process of high-temperature processing of wood were analyzed. It allows to evaluate the relationship between changes in temperature and moisture content in wood in its drying agent. In addition, some authors [21, 22] also use the capabilities of automated design when performing a related class of tasks. To conduct similar research, some authors also resort to the use of cellular automata models [7].

9. CONCLUSIONS

To summarize, this study makes a significant contribution to the field of CAD design of 3D models of drying chambers by using tools for parameterizing its geometric characteristics. At the same time, the proposed model of cellular automata provides an effective tool for modeling the drying process of hygroscopic materials in such designed 3D models of drying chambers.

The key achievement of this work is the integration of the algorithms for automated 3D design and the cellular automata model. Therefore, the developed software not only simplifies the design process, saving precious time and material resources, but also provides a powerful platform for modeling and studying the dynamics of heat and moisture transfer during the drying of hygroscopic materials.

The validation of the developed cellular automata model was carried out by comparing the obtained results with experimental data, with the average MAPE value not exceeding 13%. This level of error is acceptable, since the processes of heat and mass transfer during the drying of hygroscopic materials characterized by complexity, multifactoriality, and nonlinearity. This makes modeling with absolute accuracy impossible, even with the most advanced approaches. Under such conditions, an error of 15% considered typical for most models in this field, since achieving perfect accuracy

is extremely resource-intensive. At the same time, the proposed cellular automata model demonstrates accuracy comparable to existing models, but characterized by higher computational speed, which makes it practically valuable for real-world applications.

It is also worth noting the possibility of determining changes in the parameters of the hygroscopic material and its drying agent during the modeling process. This was realized due to the improved structure of the cellular automaton field, which takes into account the physical and geometric characteristics of the whole 3D model of the drying chamber. This field structure makes it possible to use different types of cells and the relationships between them, which are realized by the corresponding transition rules.

REFERENCES

- Sokolovskyy Y, Sinkevych O, Shymanskiy V, Boretska I, Samotii T. Construction of an asynchronous cell-automatic model for investigating the thermal mass transfer process. 2021 IEEE XVIIth Int Conf Perspect Technol Methods MEMS Des MEMSTECH 2021. 2021;29-33. Available from: <https://doi.org/10.1109/MEMSTECH53091.2021.9467930>
- Mende FF, Shurupov IA. Simple camera for high-quality wood drying. Eng Technol. 2015;2(3):95-117.
- Zhao J, Cai Y. A comprehensive mathematical model of heat and moisture transfer for wood convective drying. Holzforschung. 2017;71(5):425-35. Available from: <https://doi.org/10.1515/hf-2016-0148>.
- Kadem S, Lachemet A, Younsi R, Kocaefe D. 3D-transient modeling of heat and mass transfer during heat treatment of wood. Int Commun Heat Mass Transf. 2011;38(6):717-22. Available from: <https://doi.org/10.1016/j.icheatmasstransfer.2011.03.026>
- Ovsyak OV, Dendiuk MV. Mathematical modeling of moisture transfer in wood drying for the two-dimensional case. Sci Bull UNFU. 2023;33(4):59-64. Available from: <https://doi.org/10.36930/40330408>.
- Shumylyak L, Zhikharevych V, Ostapov S. Study of the method of asynchronous cellular automata when applied to heat conduction problems. Inf Process Syst. 2018;1(152):74-9. Available from: <https://doi.org/10.30748/soi.2018.152.11>
- Boichot R, Luo L, Fan Y. Tree-network structure generation for heat conduction by cellular automaton. Energy Convers Manag. 2009;50(2):376-86. Available from: <https://doi.org/10.1016/j.enconman.2008.09.003>.
- Sokolovskyy Y, Sinkevych O. Software for automatic calculation and construction of chamber drying wood and its components. XII Int Conf Perspect Technol Methods MEMS Des MEMSTECH. 2016;209-13. Available from: <https://doi.org/10.1109/MEMSTECH.2016.7507544>
- Chopard B, Droz M. Cellular automata modeling of physical systems. Cambridge: Cambridge University Press; 1998. Available from: <https://doi.org/10.1017/CBO9780511549755>
- Zhang J, Miao P, Zhong D, Liu L. Mathematical modeling of drying of Masson pine lumber and its asymmetrical moisture content profile. Holzforschung. 2014;68(3):313-21. Available from: <https://doi.org/10.1515/hf-2013-0077>
- Ravshanov N, Shadmanov I, Kubyashev K, Khikmatullaev S. Mathematical modeling and research of heat and moisture transfer processes in porous media. E3S Web Conf. 2021;264:01038. Available from: <https://doi.org/10.1051/e3sconf/202126401038>
- Plumb OA, Spolek GA, Olmstead BA. Heat and mass transfer in wood during drying. Int J Heat Mass Transf. 1985;28(9):1669-78. Available from: [https://doi.org/10.1016/0017-9310\(85\)90141-3](https://doi.org/10.1016/0017-9310(85)90141-3)
- Mnasri F, Abahri K, El GM, Bennacer R, Gabsi S. Numerical analysis of heat, air, and moisture transfers in a wooden building material. Therm Sci. 2017;21(2):785-95. Available from: <https://doi.org/10.2298/TSCI160421248M>
- Ovsyak OV, Dendiuk MV. Using cellular automata to simulate external heat and mass transfer in the wood drying process. Sci Bull UNFU. 2023;33(5):63-9. Available from: <https://doi.org/10.36930/40330508>.
- Hirnyk LM, et al. Mathematical modeling of convective drying processes. Budivelnik. 1993. [In Ukrainian].

16. Hirnyk LM, et al. Automation of wood drying processes in the construction industry. *Budivelnyk*. 1992. [In Ukrainian].
17. Sokolovskyy Y, Sinkevych O. Calculation of the drying agent in drying chambers. 2017 14th Int Conf Exp Des Appl CAD Syst Microelectron CADSM 2017. 2017;27-31. Available from: <https://doi.org/10.1109/CADSM.2017.7916077>
18. Ilachinski A. Cellular automata: a discrete universe. Singapore: World Scientific; 2001. Available from: <https://doi.org/10.1142/4702>
19. Sokolovskyy Y, Sinkevych O. Study of heat and mass transfer into biomaterials by using asynchronous cellular automata. 16th Int Conf Comput Sci Inf Technol CSIT 2021. 2021;274-7. Available from: <https://doi.org/10.1109/CSIT52700.2021.9648826>
20. Nearing TY, Peters-Lidard GS, Harrison CD, Tang L. Performance metrics, error modeling, and uncertainty quantification. *Mon Weather Rev*. 2016;144(2):607-13. Available from: <https://doi.org/10.1175/MWR-D-15-0087.1>
21. Li G, Li Y, Chen Q. CAD/CAE system for wooden package based on SolidWorks. *Appl Mech Mater*. 2012;(200):487-91.
22. Kyratsis P, Tzotzis A, Manavis A. Computational design and digital fabrication. *Adv Manuf Syst*. 2021;1-16.

The authors of the work would like to express special thanks to *Yuriy Guber*, PhD, Associate Professor of the Department of Environmental and Wood Protection Technologies and Life Safety of the Ukrainian National Forestry University, for the opportunity to obtain graphs of experimental data from a real drying chamber.

Yaroslav Sokolovskyy:  <https://orcid.org/0000-0003-4866-2575>

Oleksiy Sinkevych:  <https://orcid.org/0000-0001-6651-5494>



This work is licensed under the Creative Commons BY-NC-ND 4.0 license.